RETRIEVAL OF 3D-POSITION OF A PASSIVE OBJECT USING INFRARED LED'S AND PHOTODIODES

Henrik Vie Christensen

Department of Control Engineering, Aalborg University, Aalborg, Denmark, vie@control.aau.dk

ABSTRACT

A sensor using infrared emitter/receiver pairs to determine the position of a passive object is presented. An array with a small number of infrared emitter/receiver pairs are proposed as sensing part to acquire information on the object position. The emitters illuminates the object and the intensity of the light reflected by the object is measured by the receivers. The emitter/receiver pairs are fixed positioned in a 2D-plane. A model, of the light reflections from IR-emitters to IR-receivers, is used to determine the position of a ball using a Nelder-Mead simplex algorithm. Laboratory experiments show good agreement between actual and retrieved positions when tracking a ball. The ball has been successfully replaced by a human hand, and a "3D non-touch screen" with a human hand as "pointing device" is shown possible.

1. INTRODUCTION

There exists various vision based systems for determining 3D-position of objects, for instance [1] and [2]. The vision based systems have very high ratios of acquired to desired information e.g. 1000 or more. The intention with the method presented here is to make a model based position determination system based on an array of fixed positioned infrared LED and photodiodes where the ratio of acquired to desired information is much smaller, e.g. 100 or less. There exists an approach to determine position from reflection using sets of prolate spheroids with emitter and receiver in the focal points [3].

In the present study the theory of light propagation and reflection has been used to make a reflection model for an IR emitter/receiver pair [4]. This model is used together with a search algorithm to determine the 3D-position of a passive object, initially a ball. One application of this 3D position retrieval is a "3D non-touch screen" used to input 3D-positions into a computer. For this "3D non-touch screen" to be handy, pointing using a human hand would be preferable to a ball on a stick. The approach with the reflec-
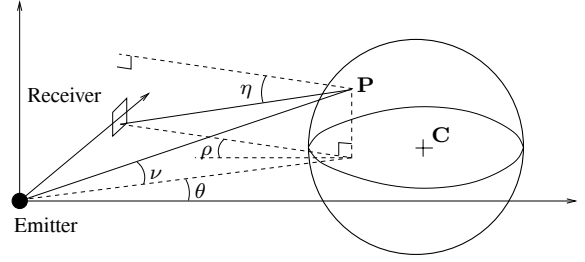
Fig. 1. The geometry of the 3D-reflection map model.

tion map may also be used to do object recognition. Object recognition is not discussed further in this paper.

2. MODEL

The model used in the 3D-position determination system is the 3D reflection map model briefly described in the following, for detail see [4]. The model of reflected light is a geometric model based on the assumption that the light source continuously emits a constant number of photons per time unit. The light source is assumed to be a point source. Fig. 1 shows the geometry of the 3D reflection map model. The light source is assumed to have an intensity characteristic denoted by $L_i(\nu, \theta, \mathbf{n}_e)$ where ν and θ are angles of direction with respect to the emitter normal $\mathbf{n}_e$. When the ball reflects light it can be considered as a light source with intensity depending on the intensity and direction of the light it reflects. The intensity of the light reaching the receiver from a single point P on the ball can then be found as

$$I_p = \int_{\mathcal{R}} m_r(P, \mathbf{n}_r) L_o(P, \phi, \rho, \eta, \mathbf{n}_r, \nu, \theta, \mathbf{n}_e)\, d\eta\, d\rho$$

where $\mathcal{R}$ is the receiver area, $\mathbf{n}_r$ is the normal vector of the receiver, m_r is the receiver characteristic, ϕ is the incidence angle at the sphere, ρ and η are the angles of direction to the receiver from the point P on the ball. Integrating over all the points in sight of both light source and the receiver gives the following equation for the intensity of the light reaching the receiver.

$$I = \int_{\mathcal{P}} I_p\, d\theta\, d\nu \qquad (1)$$

where $\mathcal{P}$ is the area on the ball that is in line of sight of both light source and receiver. The integration limits can be found from the position of ball center, ball radius and the position and direction of the light source and receiver. With a Lambertian reflection characteristic for the object, the integral equation (1) can be found to be

$$I = \frac{\rho_{\mathrm{d}}}{\pi} \int_{\nu_1}^{\nu_2} \int_{\theta_1}^{\theta_2} L_{\mathrm{i}}(\nu, \theta, \mathbf{n}_{\mathrm{e}}) \cos \phi \int_{\rho_1}^{\rho_2} \int_{\eta_1}^{\eta_2} \cos \zeta \, d\eta \, d\rho \, d\theta \, d\nu$$

For further details see [4].

3. POSITION RETRIEVAL

Based on the 3D reflection map model and measurement of light reflection from a number of emitter/receiver pairs, it is possible to search for the object position that gives reflections from the 3D reflection map model that best fits the measured reflections.

3.1. Nelder-Mead Simplex Algorithm

The Nelder-Mead simplex algorithm [5] is an algorithm for finding local minima of a function without using gradient information. The Nelder-Mead simplex algorithm is iterative each iteration follows the rules:

1. Sort. Sort the vertices of the simplex so that $f(\mathbf{x}_1) \leq f(\mathbf{x}_2) \leq \cdots \leq f(\mathbf{x}_{n+1})$.

2. Reflect. Set $\mathbf{x}_{\mathrm{r}} = (\mu_{\mathrm{r}} + 1)\bar{\mathbf{x}} - \mu_{\mathrm{r}}\mathbf{x}_{n+1}$, where $\bar{\mathbf{x}} = \frac{1}{n} \sum_{i=1}^{n} \mathbf{x}_i$ is the centroid of the convex hull of the n best points. Compute $f_{\mathrm{r}} = f(\mathbf{x}_{\mathrm{r}})$. If $f(\mathbf{x}_1) \leq f_{\mathrm{r}} \leq f(\mathbf{x}_n)$ then set $\mathbf{x}_{n+1} = \mathbf{x}_{\mathrm{r}}$ and terminate the iteration.

3. Expand. If $f_{\mathrm{r}} < f(\mathbf{x}_1)$ compute $\mathbf{x}_{\mathrm{e}} = (\mu_{\mathrm{e}} + 1)\bar{\mathbf{x}} - \mu_{\mathrm{e}}\mathbf{x}_{n+1}$ and $f_{\mathrm{e}} = f(\mathbf{x}_{\mathrm{e}})$. If $f_{\mathrm{e}} < f_{\mathrm{r}}$ then set $\mathbf{x}_{n+1} = \mathbf{x}_{\mathrm{e}}$; otherwise, set $\mathbf{x}_{n+1} = \mathbf{x}_{\mathrm{r}}$ and terminate the iteration.

4. Outside Contraction. If $f(\mathbf{x}_n) \leq f_{\mathrm{r}} < f(\mathbf{x}_{n+1})$ compute $\mathbf{x}_{\mathrm{oc}} = (\mu_{\mathrm{oc}} + 1)\bar{\mathbf{x}} - \mu_{\mathrm{oc}}\mathbf{x}_{n+1}$ and $f_{\mathrm{c}} = f(\mathbf{x}_{\mathrm{oc}})$. If $f_{\mathrm{c}} < f_r$ set $\mathbf{x}_{n+1} = \mathbf{x}_{\mathrm{oc}}$ and terminate the iteration; otherwise, go to step 6.

5. Inside Contraction. If $f_{\mathrm{r}} \geq f(\mathbf{x}_{n+1})$ compute $\mathbf{x}_{\mathrm{ic}} = (\mu_{\mathrm{ic}} + 1)\bar{\mathbf{x}} - \mu_{\mathrm{ic}}\mathbf{x}_{n+1}$ and $f_{\mathrm{c}} = f(\mathbf{x}_{\mathrm{ic}})$. If $f_{\mathrm{c}} < f(\mathbf{x}_{n+1})$ set $\mathbf{x}_{n+1} = \mathbf{x}_{\mathrm{ic}}$ and terminate the iteration.

6. Shrink. For $2 \leq i \leq n+1$ set $\mathbf{x}_i = \mathbf{x}_1 - (\mathbf{x}_i - \mathbf{x}_1)/2$; compute $f(\mathbf{x}_i)$.

The constants are $\mu_{\mathrm{r}} = 1$, $\mu_{\mathrm{e}} = 2$, $\mu_{\mathrm{oc}} = \frac{1}{2}$ and $\mu_{\mathrm{ic}} = -\frac{1}{2}$. Fig. 2 shows the Simplex and the possible new points for the Nelder-Mead simplex algorithm (in 2 dimensions).

Exit the iterations when either $\max |f(\mathbf{x}_i) - f(\mathbf{x}_1)| < \epsilon_{\mathrm{f}}$ or $\max \|\mathbf{x}_i - \mathbf{x}_1\| < \epsilon_{\mathrm{x}}$ for $i = 2, \ldots, n+1$.
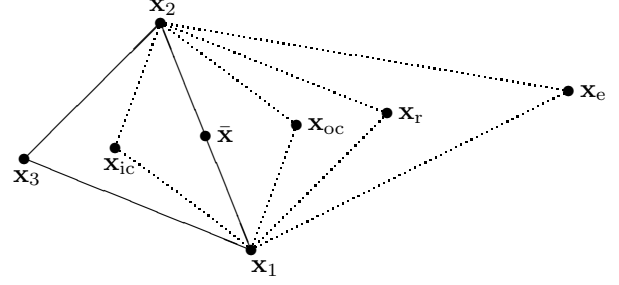

Fig. 2. Nelder-Mead simplex and new points

When the Nelder-Mead simplex algorithm terminates in step 2 one function evaluation is needed, termination in step 6 requires at most $4 + n$ function evaluations. The computational time for finding an approximate minimum of the function f can thus be bounded by limiting the number of function evaluations allowed. See e.g. [6] for a more detailed description of the Nelder-Mead Algorithm.

3.2. Applying the Nelder-Mead Simplex Algorithm to Track an Object

To use Nelder-Mead simplex algorithm for determining the position of the object, setup the simplex in the parameter space for the reflection map model, that is (x, y, z) coordinates for the ball center. Experiments has shown that an appropriate starting point is the center of the measurable volume and a simplex size of 1.5. The function to be minimized by the Nelder-Mead simplex algorithm is the Euclidean distance between measured and modeled reflections. When the Nelder-Mead simplex algorithm terminates, $\mathbf{y} = \mathbf{x}_1$ is the estimated object position.

For the second position retrieved start with the first position found, and the same simplex size. For the next positions, the starting position is predicted linearly from the two previous retrieved positions as $\mathbf{s}_i = \mathbf{y}_{i-1} + (\mathbf{y}_{i-1} - \mathbf{y}_{i-2})$. The simplex size is set to $\max(0.05, 0.1\|\mathbf{y}_{i-1} - \mathbf{y}_{i-2}\|)$.

4. MEASUREMENTS

4.1. Physical Setup

The physical setup for laboratory measurements for validating the 3D position retrieval consists of eight infrared sensors each with one emitter (SFH485P) and one receiver (BF104F), a positioning device for moving the ball, and a computer with an acquisition interface. The sensors are placed on the boarder of a computer monitor, four in the corners and four on the halfway on each side. They are directed towards a point 15cm in front of the screen center. The computer used is a dual Pentium, 700MHz, with NI-DAQ sampling cards (PCI-6071E and 6713).

IV - 1094

4.2. Simultaneous Measurement of Reflections

Appropriate modulation of the light emitted from the individual emitters makes it possible to measure simultaneous for all emitter/receiver pairs. To minimize the disturbance from frequency localized disturbances e.g. artificial lighting Rudin-Shapiro sequences are chosen for modulation. The symmetric Rudin-Shapiro transform [3, 7] is used to construct orthogonal spread spectrum signals. Other types of modulation e.g. waveletpackage could also be used [3, 7]. The Rudin-Shapiro sequences have the advantage of taking only the discrete values ± 1 and the Rudin-Shapiro transform is it's own inverse. The orthogonality property makes it easy to separate signals from each emitter using inner products. With the 16 bit Rudin-Shapiro sequence modulation used, the hardware is capable of measuring reflections on all 64 (8×8) channels with a rate of $200 Hz$.

For the 3D position retrieval only 34 of the 64 possible emitter/receiver pairs are used, leaving the most distant pairs out. Using all sensor pairs gives degraded results due to low signal to noise ratio for the most distanced emitter/receiver pairs.

To reduce disturbances on the reflection measurements, the background reflections are measured and subtracted. The Rudin-Shapiro sequence used is length 16 giving 16 measurement channels. Eight of these are used for measuring reflections, the remaining are used to measure the DC-offset and noise, the DC-offset is then subtracted. Further more averaging over a number of measured reflection intensities is used to reduce the random noise.

4.3. Fitting the Model

The model is calibrated by measuring the reflections from the ball positioned in a 3D-grid of $21 \times 18 \times 17$ equidistantly spaced points in front of the sensor arrangement. For each position average over 100 reflection measurements are made to reduce noise. The measurements are then used to find the model parameters by minimizing for each emitter/receiver pair

$$e = \sum_{\mathbf{c} \in X} (I_{\mathrm{m}}(\mathbf{c}, E_{\mathrm{m}}, R_{\mathrm{m}}) - \max(rI(\mathbf{c}, E, R), I_{\mathrm{sat}}))^2$$

over r, E_m and R_m, where r is a scalar to compensate for various gains in the physical setup (e.g. ρ_d and receiver amplification), E_m and R_m is emitter and receiver position and orientation in the model respectively, $\mathbf{c}$ is the ball position, $I(\mathbf{c}, E, R)$ is the measured reflections from the ball at position $\mathbf{c}$ and I_{sat} is the level where the receiver saturates.

5. RESULTS

The 3D position retrieval is tested by measuring the reflections from the ball positioned along a curve, and then using
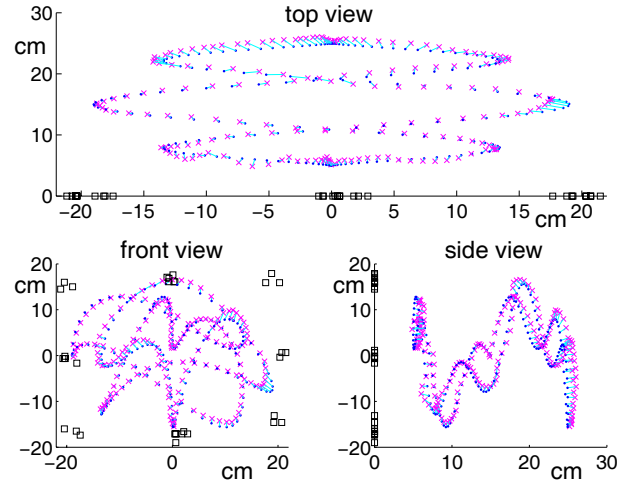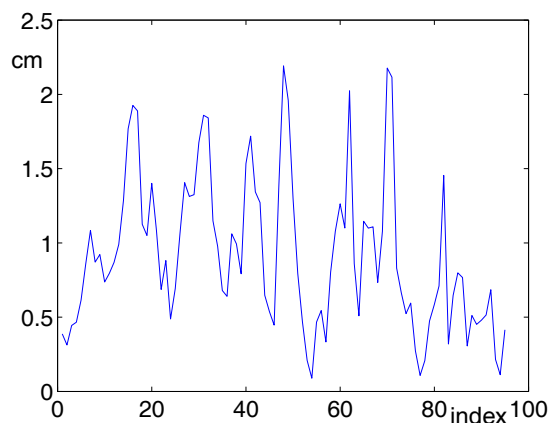

Fig. 3. Actual ball positions (dots) and retrieved positions (x-marks), pair vise connected by a line. Axis units are cm.

the Nelder-Mead simplex algorithm to search for the best fitting 3D position in the Reflection Map Model. The maximal number of function (model) evaluation has been limited to 70, trade off between computation time and approximation accuracy. Fig. 3 shows top, front and side view of both retrieved positions (x-marks) and actual ball position (dots), the actual ball position are connected to the corresponding retrieved position to show the alignment. The axis units on the figure are centimeters. As the figures shows the retrieved positions are close to the actual ones. Fig. 4 shows the distance between actual ball position and retrieved position, y axis is centimeters and x axis is position index. The retrieved position is seen to be within 2.2cm from the actual position. Fig. 5 shows the misalignment if the ball had been moving twice as fast (every 2'nd point used) along the curve. Still with distance between actual and retrieved po-
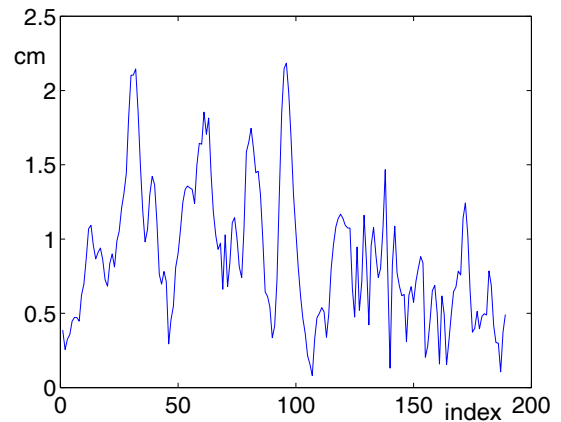
Fig. 4. The distance between actual ball positions and retrieved positions. x axis is position index, y axis is cm.

IV - 1095

Fig. 5. The distance between actual ball positions and retrieved positions. x axis is position index, y axis is cm.
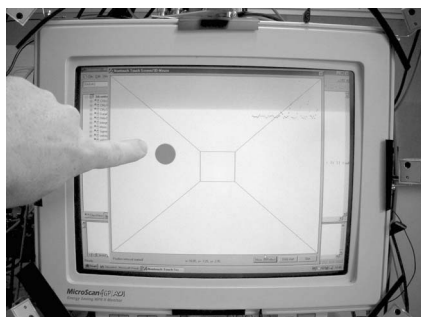
Fig. 6. The "non-touch" screen with the hand close to the screen.

sition below 2.2cm.

Using the same setup, but with a hand as pointing device, it is possible to make a "3D non-touch screen". The precision of the 3D-position detected degrades slightly due to disturbance reflections from the human arm, and only averaging over 38 measurements. With the hardware used the 3D positions can be obtained with a rate of $5Hz$.
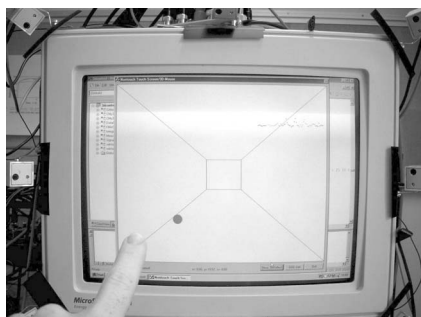
Fig. 7. The "non-touch screen" with the hand distant from the screen.

Fig. 6 and Fig. 7 shows photos of the "non-touch screen".

The courser on the screen is a disc, that changes size depending on the depth coordinate i.e. when the hand is close to the screen a big disc is shown and when the hand is further from the screen a smaller disc is shown.

6. CONCLUSION

A method for retrieving the 3D-position of a passive object using infrared LED's and photodiobes, based on the 3D reflection map model and the Nelder-Mead simplex algorithm has been proposed. Experiments in the laboratory has shown that the method is successful. When applied to measured reflections from the ball, sufficient information is obtained to find the 3D-position of that ball is obtained. The method has shown robustness against replacing the ball by a human hand, though the precision degrades slightly because of disturbances from the human arm. Despite this degradation in precision, the method have shown promising results in the "3D non-touch screen" experiments. To improve performance of the "3D non-touch screen" further investigation is planned to make an intelligent selection on which channels to include in the 3D-position determination process.

7. REFERENCES

[1] C. Jennings, "Robust finger tracking with multiple cameras," in *Proc. Int. Workshop on Recognition, Analysis and Tracking of Faces and Gestures in Real-Time Systems*, Sept. 1999, pp. 152–160.

[2] J.M. Rheg and T. Kanade, "Digiteyes: vision-based hand tracking for human-computer interaction," in *Proc. of the IEEE Workshop on Motion of Non-rigid and Articulated Objects*, Nov. 1994, pp. 16 –22.

[3] A. la Cour-Harbo, *Robust and Low-Cost Active Sensors by means of Signal Processing Algorithms*, Ph.D. thesis, Aalborg University, Aug. 2002, ISBN 87-90664-13-2.

[4] H.V. Christensen, "3d reflection map modeling for optical emitter-receiver pairs," in *Proc. of IEEE Sensors*, Oct. 2004, To apear.

[5] J.A. Nelder and R. Mead, "A simplex method for function minimization," *J. Computer*, vol. 7, no. 4, pp. 308–313, 1965.

[6] C.T. Kelly, *Iterative Methods for Optimization*, Frontiersin Applied Mathematics. SIAM, 1999, ISBN 0-89871-433-8.

[7] A. la Cour-Harbo and J. Stoustrup, "Using spread spectrum transform for fast and robust simultaneous measurement in active sensors with multiple emitters," in *Proc. of IECON 02*, Nov. 2002, vol. 4, pp. 2669–2674.